



---

## Effect of Annealing Process on Porous Aluminium Filled with Graphite

Amel Lafi Al-Otaibi<sup>1</sup>, Muneera Abdullah Al-messiere<sup>1</sup> and Taher Ghrib<sup>1,2\*</sup>

<sup>1</sup>Laboratory of Physical Alloys (LPA), Science Faculty of Dammam, Dammam University, Saudi Arabia.

### Authors' contributions

*This work was carried out in collaboration between all authors. They have designed, managed the analyses and literature search and finally read and approved the final manuscript.*

**Short Communication**

Received 20<sup>th</sup> February 2014  
Accepted 22<sup>nd</sup> April 2014  
Published 10<sup>th</sup> June 2014

---

### ABSTRACT

Thermal properties of porous thin films formed by anodization of thin aluminum films in sulfuric acid. The obtained pores at the surface are filled by sprayed graphite which the role is to improving its optical and thermal absorption giving a structure of an assembly of three different media such as graphite/(Porous aluminium layer filled with graphite)/(Al sample). The realized structure is annealed in temperature range varying from the room temperature to 650°C for various durations. Thermal properties of the realized structure was studied by Photothermal Deflection (PTD) Technique and correlated to the microstructure evolution. It was found that this structure is characterised by thermal conductivity which, conversely to thermal diffusivity, increases with the heating duration and temperature in the furnace and can be used in solar energy field.

*Keywords: Porous aluminum; absorption coefficient; PTD technique; thermal conductivity.*

### 1. INTRODUCTION

In view of their practical importance, aluminium porous materials were intensively studied in the last decades [1-11] with various analytical techniques. They have considerable interest primarily for the reason of its self organized pores and for its quasi-cylindrical and aligned

---

\*Corresponding author: Email: [taher.ghrib@yahoo.fr](mailto:taher.ghrib@yahoo.fr);

pores with sizes in the vicinity of nanometers ranges and this properties constitute a technological revolution and find now many applications such as filtration membranes [12,13], as backing of fabrication nanowires [14-16], as photonic crystals [17,18], as humidity sensors [19,20], or as cathodes for organic light emitting diodes [21,22]. The scientists have been focused on the fabrication of organized nano-pores by electrochemical methods by simple variation of the anodization parameters, such as voltage and electrolyte solution composition. In the literature many attempt are reported in order to find relationships between porosity, thermal properties [23,24], optical properties [11,25,26], and this by exploring the effect of size, form and density of the pores. For photovoltaic applications knowing sample emissivity, absorption and thermal properties is a primordial issue for solar energy development. The aim of this work is to present a method for the fabrication of ordered nanopores on aluminum substrate and to study the influence of heat treatment parameters such as the annealing temperature and heating duration on thermal properties such as thermal conductivity and thermal diffusivity which are determined by the photothermal deflection (PTD) technique [27-29].

## 2. EXPERIMENTS

Aluminum foil with high purity foil (99.997%), 0.25 mm thick was used as a starting material. The cleaned samples were anodized during 25 min in a solution of dilute sulphuric acid with 66.66%  $H_2SO_4$  and 33.33%  $H_2O_2$  at room temperature and with anodization currents (200mA) at a constant potential of 28 V. A self procedure constituted with two steps of the anodization process was used for fabricating the anodic porous aluminium films, In a first step twelve pieces are cut with 50mm×50mm dimensions, which are treated by a mechanical polishing with polishing machine model 920 working with different speed combined with a alumina abrasive in an alkaline solution and in second step are cleaned by acetone and ethanol in teflon bath each one during 10 min at room temperature. Important parameters such as pore size, density and thickness of the layer can be easily controlled by the anodic voltage [2,12,17]. A classical preparation method including a mechanical fixation of the samples in a standard 3 mm ring followed by mechanical thinning of samples down to 50  $\mu m$  has been used.

The thermal properties such as the thermal conductivity and the thermal diffusivity are determined by the PTD technique. This method (Fig. 1) consists in heating the sample with a modulated light beam of intensity  $I = I_0(1 + \cos \omega t)$  that will be absorbed on the surface and generates a thermal wave. This thermal wave will propagate in the sample and in the surrounding fluid (air in our case) and will induce a temperature gradient and then a refractive index gradient in the fluid. The fluid index gradient will cause the deflection  $\psi$  of a probe laser beam skimming the sample surface. This deflection may be related to the thermal properties of the sample. The sample is heated by a halogen lamp light of Power 100W modulated by using a mechanical chopper at a variable frequency. A (He-Ne) laser beam skimming the sample surface at a distance  $x$  is deflected. This deflection can be detected by a four quadrant photo-detector and converted to an electrical signal which is measured by a lock-in amplifier. Through the intermediary of interfaces, mechanical chopper and Lock-in amplifier a microcomputer will set the desired modulation frequency and read the values of the amplitude and phase of the photo-thermal signal and then draw their variations according to the square root modulation frequency.

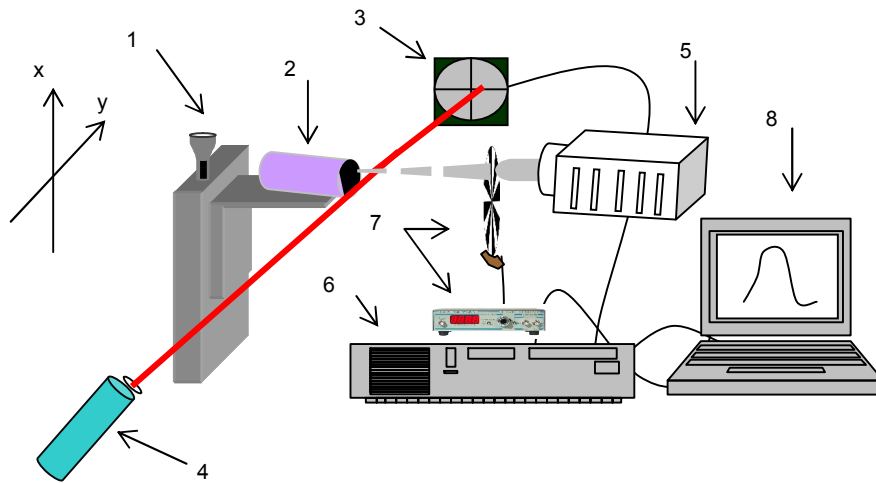


**Fig. 1. Experimental set-up used for PTD investigation: 1-Table of horizontal and vertical micrometric displacement, 2-Sample, 3-Photodetector position, 4-Fixed laser source, 5-Halogen lamp, 6-Look-in amplifier, 7-Mechanical chopper, 8-Computer**

After obtaining the porous Al, the sample is covered with a graphite layer and heated in a furnace of a control temperature for different durations giving a sample consisting of a stack of three layers (Fig. 2). The deposited graphite on the substrate is used in order to absorb the totality of incident light and thus playing the role of a heat source which is characterized by a thermal conductivity  $K_1=0.35W.m^{-1}.K^{-1}$  and a thermal diffusivity  $D_1 = 1.45 \times 10^{-6} m^2.s^{-1}$  [28].

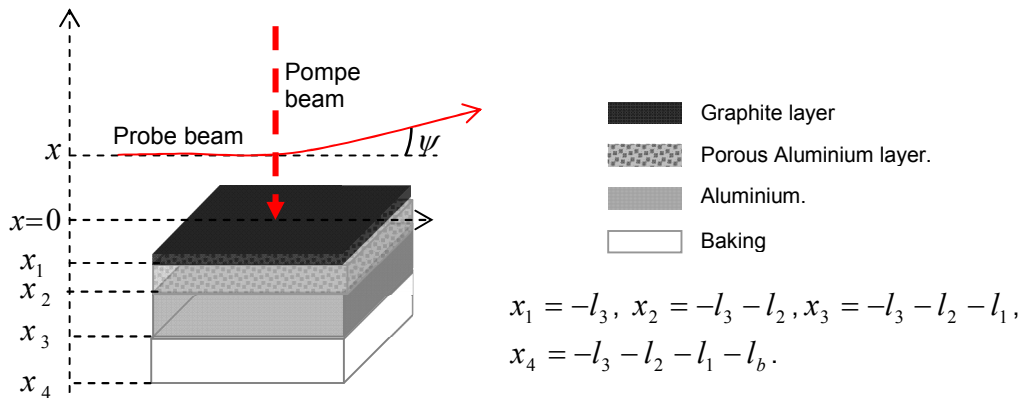


**Fig. 2. Schema of the stacked three layers**

### 3. RESULTS AND DISCUSSION

Fig. 3 shows AFM images of the top surface morphology of porous aluminum film formed in sulfuric acid and annealed in 300°C, 350°C and 400°C for 20 min duration. The diameter of the nano-pores is estimated to vary from 40 to 100 nm, whose depth is of the order of 5

microns, which varies with the anodizing parameters [11,30] and for the same heating duration decrease with annealing temperature and whose density increases.

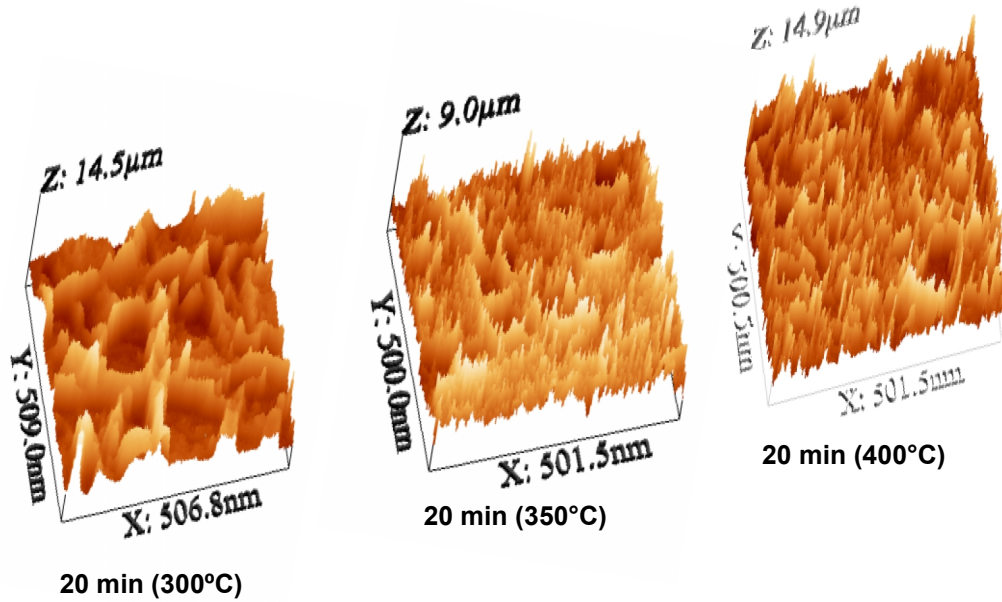


**Fig. 3. AFM micrograph of porous Al layer film formed in sulfuric acid by two step anodization process annealed in 300°C, 350°C and 400°C for 20 min duration.**

To determine the thermal properties of the samples, the photothermal deflection model in the case of a uniform heating with one-dimensional approximation is used. The amplitude  $|\psi|$  and phase  $\varphi$  of the probe beam deflection  $\psi$  are then given in this case by [28,29]:

$$|\psi| = \frac{\sqrt{2} L}{n \mu_f} \frac{dn}{dT_f} |T_0| e^{-\frac{x}{\mu_f}} \quad \text{and} \quad \varphi = -\frac{x}{\mu_f} + \theta + \frac{5\pi}{4}$$

Where  $L$  is the width of the pump beam in the direction of the probe laser beam,  $n$ ,  $\mu_f$  and  $T_f$  are respectively the refractive index, the thermal diffusion length and the temperature of the fluid.  $|T_0|$  and  $\theta$  are respectively the amplitude and phase of the temperature  $T_0$  at the sample surface which are function of the thermal properties of the different media.  $x$  is the distance between the probe beam axe and the sample surface.

Before the calculation of the probe beam deflection, one must know the expression of the surface temperature  $T_0$  which is calculated by writing the heat flow and temperature

continuity at the interfaces  $x_1 = -l_3$ ,  $x_2 = -l_3 - l_2$ ,  $x_3 = -l_3 - l_2 - l_1$  which gives the following expression: [29]

$$T_0 = \left[ \left( (1+b)\eta_4 e^{\sigma_1 l_1} - (1-b)\eta_2 e^{-\sigma_1 l_1} \right) E_3 + (r_1 - b) e^{-\alpha_1 l_1} E_1 \right] / \left[ (1-b)\eta_1 e^{-\sigma_1 l_1} - (1+b)\eta_3 e^{\sigma_1 l_1} \right]$$

Where  $\eta_1, \eta_2, \eta_3, \eta_4, b, \sigma_1, r_1, E_1$  and  $E_3$  are real or complex parameters [29], which depend on the optical and thermal properties of different layers.

In order to determine the thermal properties evolutions with the annealing temperature a study of the photothermal signal with the square root modulation frequency is carried out for different samples treated with various annealing temperatures and for various durations.

The experimental evolution of the normalised amplitude (by dividing the amplitude by its maximum value) and phase of the photothermal signal with the square root modulation frequency for the investigated samples annealed respectively at 300°C, 350°C and 400°C and maintained in the furnace for 20, 30, 45 and 55 min are given in Figs. 4-6.

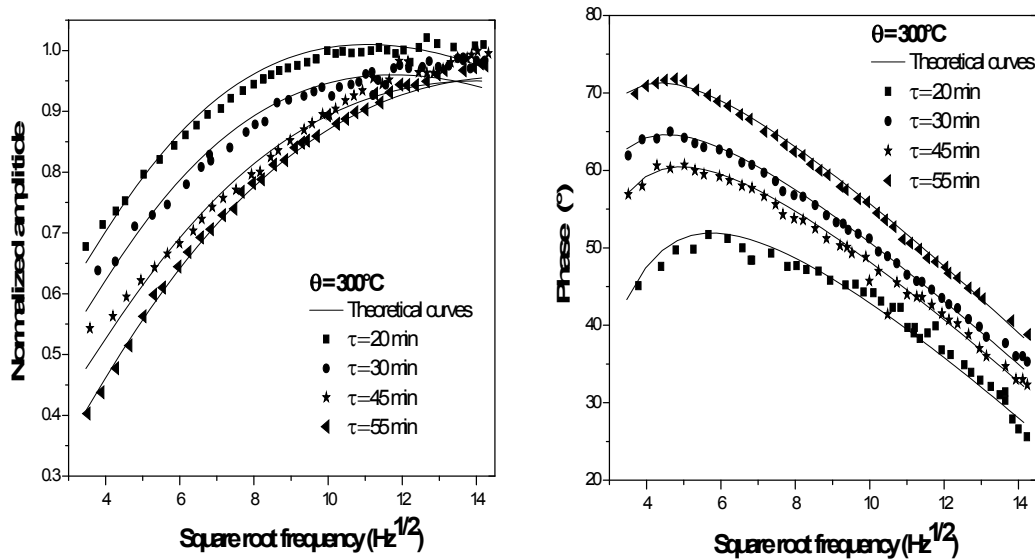


**Fig. 4. Experimental and theoretical amplitudes and phase signals versus the square root modulation frequency of the porous aluminum annealed at 300°C temperature for 20, 30, 45 and 55min durations**

Each sample is composed of a succession of three layers (Fig. 2), a thick layer of the brut aluminium, the porous aluminium layer filled of graphite (PAG) with thickness of  $l_2 = 15 \mu m$  and the graphite layer with thickness of  $l_3 = 6 \mu m$ . In this experience temperature range, the aluminium does not change its thermal properties, and then the variations in the photothermal signal are due essentially to the change of the thermal properties of the PAG layer.

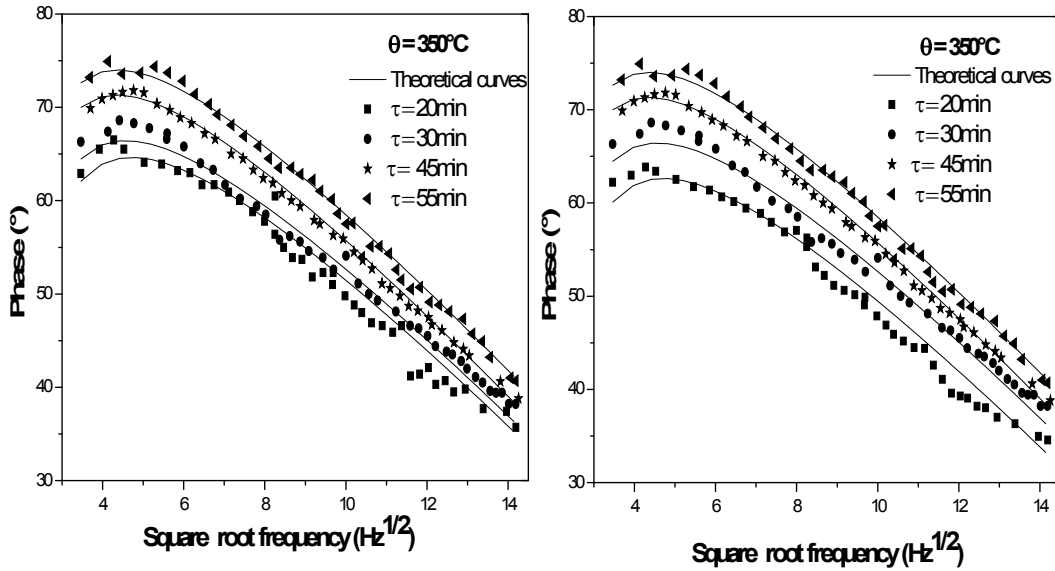


Fig. 5. Experimental and theoretical amplitudes and phase signals versus the square root modulation frequency of the porous aluminum annealed at  $350^\circ\text{C}$  temperature for 20, 30, 45 and 55min durations

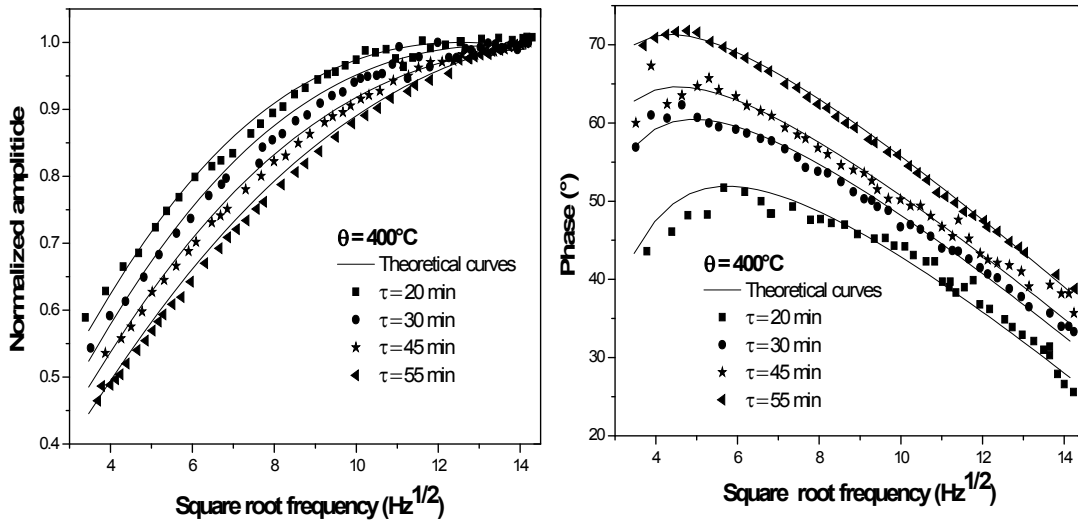
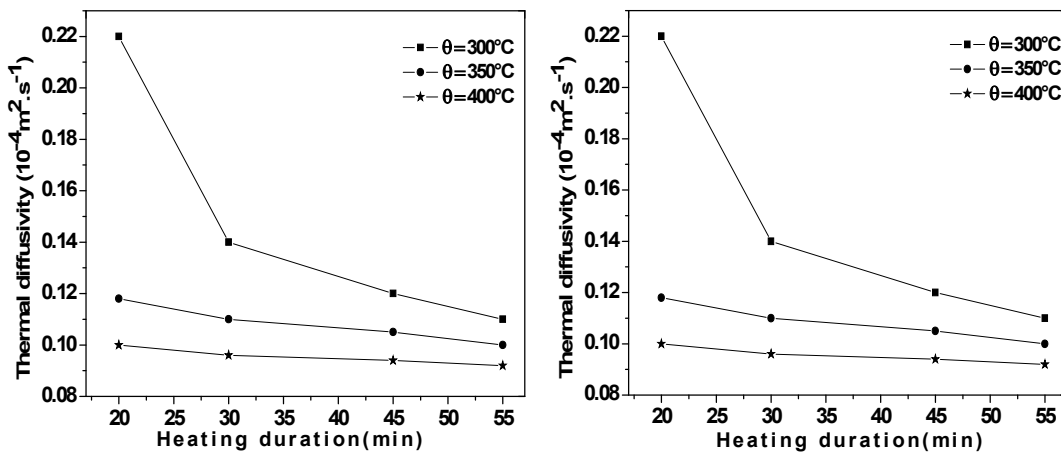


Fig. 6. Experimental and theoretical amplitudes and phase signals versus the square root modulation frequency of the porous aluminum annealed at  $400^\circ\text{C}$  temperature for 20, 30, 45 and 55min durations

We use the model of three layers previously developed by taking  $K_3 = 278 \text{ W.m}^{-1}.\text{K}^{-1}$  and  $D_3 = 0,96 \times 10^{-4} \text{ m}^2.\text{s}^{-1}$  of the aluminium, and thermal properties of the graphite layer having values  $K_1 = 0,35 \text{ W.m}^{-1}.\text{K}^{-1}$  and  $D_1 = 1,45 \times 10^{-6} \text{ m}^2.\text{s}^{-1}$  [14].

The thermal conductivity  $K_2$  and the thermal diffusivity  $D_2$  of the PAG layer are determined by comparing the experimental amplitude and phase curves to the corresponding theoretical ones. The best theoretical fitting between the experimental and theoretical curves gives the values of the couple  $(K_2, D_2)$ .

After simulations of the curves of Figs. 4-6 one obtains Fig. 7 which gives the evolution of the thermal conductivity  $K_2$  and the thermal diffusivity  $D_2$  of the PAG layer versus the soaking time for different annealing temperature, provides that the thermal conductivity conversely to the thermal diffusivity, increases with the heating time and annealing temperature.



**Fig. 7. Evolution of the thermal conductivity and thermal diffusivity of the porous aluminum doped with the graphite versus the soaking duration and annealing temperature**

Physically the thermal conductivity and the thermal diffusivity mean respectively the ability to conduct the heat and the heat propagation velocity in the material. In our case we have established a material of high thermal conductivity and low thermal diffusivity. These PAL materials can be used in the solar cells and heater exchangers which require materials of great absorption coefficient, high thermal conductivity and with low diffusion speed i.e. low thermal diffusivity. If we represent the report  $\frac{K}{D} = \rho c$  ( $\rho$  and  $c$  are respectively the density and specific heat) according to the heating durations for various annealing temperatures we obtain the curves on Fig. 8.

We note that the product  $\rho c$  increases with the annealing temperature and the heating duration, this increase is essentially due to the decrease of pores dimensions which are closed gradually and tends to being constant for high annealing temperatures and long

heating durations. This material is characterized by good thermal and structural properties; it can be used in solar cells for water storage and heating.

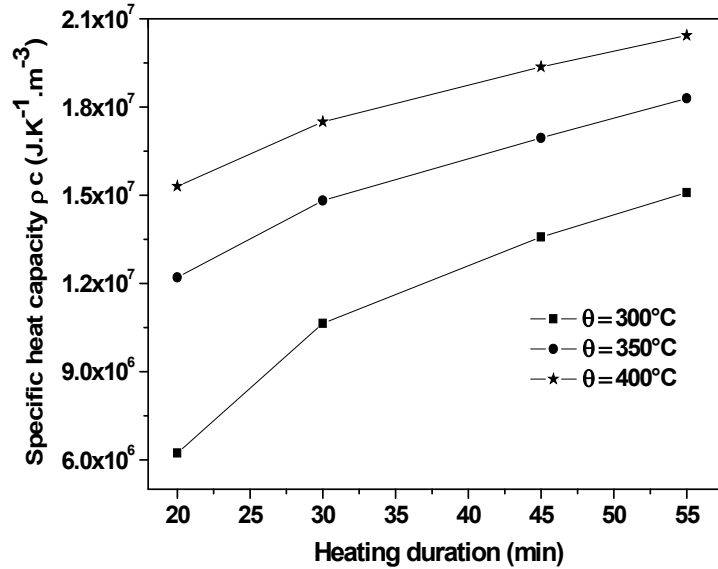


Fig. 8. Specific heat evolution versus the heating duration for various annealing temperature

#### 4. CONCLUSION

In this work investigations of thermal properties of intrinsic porous aluminum samples presenting ordered nano-pores having a diameter around 40 nm have been made. After filling these pores with black graphite and annealing it at different temperatures with different durations gives that the thermal conductivity, contrary to the thermal diffusivity, increases. The thermal properties are determined using the photothermal deflection technique which permits also to calculate the specific heat coefficient and can be related to the pores density in the obtained porous aluminum layer which decreases with the annealing temperature. The obtained material can be used in the fields of energy production and storage.

#### ACKNOWLEDGMENTS

The authors are pleased to acknowledge the financial support of this study by the Scientific Research Deanship of Dammam University, under Project no. 2013196.

#### COMPETING INTERESTS

Authors have declared that no competing interests exist.

#### REFERENCES

1. Nielsch K, Choi J, Schwirn K, Wehrspohn RB, Gosele U. Self-ordering regimes of porous alumina: The 10% porosity rule. *Nano Lett.* 2002;2:677.



2. Vrublevsky I, Parkoun V, Schreckenbach J, Marx G. Effect of the current density on the volume expansion of the deposited thin films of aluminium during porous oxide formation. *Applied Surface Science*. 2003;220(1–4):51-59.
3. Galca AC, Kooij ES, Wormeester H, Salm C. Structural and optical characterization of porous anodic aluminum oxide. *Journal of Applied Physics*. 2003;94:7.
4. Tseng WJ, Tsai CJ. Microporous layer structure in oxidized aluminium nitride polycrystals. *Journal of Materials Processing Technology*. 2004;146(3):289-293.
5. Ram J, Singh R. Effective thermal conductivity of highly porous two-phase systems. *Applied Thermal Engineering*. 2004;24:2727–2735.
6. Ku AY, Taylor ST, Heward WJ, Denault L, Loureiro SM. Heterogeneous mesoporous oxides grown in porous anodic alumina. *Microporous and Mesoporous Materials*. 2006;88(1–3):214-219.
7. Samantray PK, Karthikeyan P, Reddy KS. Estimating Effective thermal conductivity of two-Phase materials. *International Journal of Heat and Mass Transfer*. 2006;49:4209–4219.
8. Wang TC, Fan TX, Zhang D, Zhang GD, Xiong DS. Thermal conductivity and thermal expansions of aluminum/carbon composites based on wood templates. *Materials Letters*. 2007;61:1849–1854.
9. Alinejad B, Zakeri M. A novel single-step method for fabrication of dense surface porous aluminum. *Journal of Materials Processing Technology*. 2009;209(11):5042-5045.
10. Murphey MB, Bergeson JD, Etzkorn SJ, Qu L, Li L, Dai L, Epstein AJ. Spin-valve behavior in porous alumina-embedded carbon nanotube array with cobalt nanoparticle spin injectors. *Synthetic Metals*. 2010;160(3–4):235-237.
11. Ghrib M, Gaidi M, Khedher N, Ghrib T, Ben Salem M, Ezzaouia H. Structural and optical properties study of nanocrystalline Si (nc-Si) thin films deposited on porous aluminum by plasma enhanced chemical vapor deposition. *Applied Surface Science*. 2011;257(9):3998-4003.
12. Liu W, Canfield N. Development of thin porous metal sheet as micro-filtration membrane and inorganic membrane support. *Journal of Membrane Science*. 2012;409–410:113-126.
13. Barbosa EF, Silva LP. Nanoscale characterization of synthetic polymeric porous membranes: Scrutinizing their stiffness, roughness and chemical composition. *Journal of Membrane Science*. 2012;407–408:128-135.
14. Grzegorz D, Sulka, Agnieszka Brzózka, Lifeng Liu. Fabrication of diameter-modulated and ultrathin porous nanowires in anodic aluminum oxide templates. *Electrochimica Acta*. 2011;56(14):4972-4979.
15. Wang X, Li C, Chen G, He L, Cao H, Zhang B. Selective fabrication of Cu/Cu<sub>2</sub>O nanowires using porous alumina membranes in acidic solution. *Solid State Sciences*. 2011;13(1):280-284.
16. Huang J, Ren H, Sun P, Gu C, Sun Y, Liu J. Facile synthesis of porous ZnO nanowires consisting of ordered nanocrystallites and their enhanced gas-sensing property. *Sensors and Actuators B: Chemical*. 2013;188:249-256.
17. Hu X, Pu YJ, Ling ZY, Li Y. Coloring of aluminum using photonic crystals of porous alumina with electrodeposited Ag. *Optical Materials*. 2009;32(2):382-386.
18. Kurbanov SS, Shaymardanov ZSH, Kasymdzhanov MA, Khabibullaev PK, Kang TW. The luminescence of organic dye in nanocomposites based on synthetic opal and porous aluminum oxide. *Optical Materials*. 2007;29(9):1177-1182.
19. Almasi Kashi M, Ramazani A, Abbasian H, Khayyatian A. Capacitive humidity sensors based on large diameter porous alumina prepared by high current anodization. *Sensors and Actuators A: Physical*. 2012;174:69-74.

20. Juhász L, Mizsei J. Humidity sensor structures with thin film porous alumina for on-chip integration. *Thin Solid Films*. 2009;517(22):6198-6201.
21. Kukhta AV, Gorokh GG, Kolesnik EE, Mitkovets AI, Taoubi MI, Koshin YUA, Mozalev AM. Nanostructured alumina as a cathode of organic light-emitting devices. *Surface Science*. 2002;507–510:593-597.
22. Kim KP, Lee KS, Kim TW, Woo DH, Kim JH, Seo JH, Kim YK. Enhancement of the light extraction efficiency in organic light emitting diodes utilizing a porous alumina film. *Thin Solid Films*. 2008;516(11):3633-3636.
23. Wang TC, Fan TX, Zhang D, Zhang G, Xiong DS. Thermal conductivity and thermal expansions of aluminum/carbon composites based on wood templates. *Materials Letters*. 2007;61(8–9):1849-1854.
24. Dyga R, Witczak S. Investigation of Effective Thermal Conductivity Aluminum Foams. *Procedia Engineering*. 2012;42:1088-1099.
25. Zhuo H, Peng F, Lin L, Qu Y, Lai F. Optical properties of porous anodic aluminum oxide thin films on quartz substrates. *Thin Solid Films*. 2011;519(7):2308-2312.
26. Stojadinovic S, Nedic Z, Belca I, Vasilic R, Kasalica B, Petkovic M, Zekovic LJ. The effect of annealing on the photoluminescent and optical properties of porous anodic alumina films formed in sulfamic acid. *Applied Surface Science*. 2009;256(3):763-767.
27. Bertolotti M, Liakhou GL, Ferrari A, Ralchenko VG, Smolin AA, Obrastsova E, Korotoushenko KG, Pimenov SM, Konov VI. Measurements of thermal conductivity of diamond films by photothermal deflection technique. *J Appl Phys*. 1994;75:7795-7798.
28. Ghrib T, Bejaoui F, Hamdi A, Yacoubi N. *Thermochimica Acta*. 2008;473:86–91.
29. Ghrib T, Gaied I, Yacoubi N. *Nondestructive Testing: Methods, Analyses and Applications, Measurements of thermal conductivity of diamond films by photothermal deflection technique*, eBooks. Nova Publishers. 2010;95-146.
30. Ghrib M, Gaidi M, Ghrib T, Khedher N, Ben Salam M, Ezzaouia H. Morphological and optical properties changes in nanocrystalline Si (nc-Si) deposited on porous aluminum nanostructures by plasma enhanced chemical vapor deposition for Solar energy applications. *Applied Surface Science*. 2011;257(21):9129-9134.

© 2014 Al-otaibi et al.; This is an Open Access article distributed under the terms of the Creative Commons Attribution License (<http://creativecommons.org/licenses/by/3.0>), which permits unrestricted use, distribution, and reproduction in any medium, provided the original work is properly cited.

*Peer-review history:*

*The peer review history for this paper can be accessed here:*  
<http://www.sciencedomain.org/review-history.php?iid=533&id=33&aid=4867>